

THE SELF-LINKING NUMBER IN ANNULUS AND PANTS OPEN BOOK DECOMPOSITIONS

KEIKO KAWAMURO AND ELENA PAVELESCU

ABSTRACT. We find a self-linking number formula for a given null-homologous transverse link in a contact manifold that is compatible with either an annulus or a pair of pants open book decomposition. It extends Bennequin's self-linking formula for a braid in the standard contact 3-sphere.

1. INTRODUCTION

Alexander's theorem [1] states that every closed and oriented 3-manifold admits an open book decomposition.

Definition 1.1. Let Σ be a surface with non empty boundary and ϕ be a diffeomorphism of the surface fixing the boundary pointwise. We construct a closed manifold

$$M_{(\Sigma, \phi)} = \Sigma \times [0, 1] / \sim$$

where “ \sim ” is an equivalence relation satisfying $(\phi(x), 0) \sim (x, 1)$ for $x \in \text{Int}(\Sigma)$ and $(x, \tau) \sim (x, 1)$ for $x \in \partial\Sigma$ and $\tau \in [0, 1]$. The pair (Σ, ϕ) is called an *abstract open book decomposition* of the manifold $M_{(\Sigma, \phi)}$.

Alternatively, an *open book decomposition* for M can be defined as a pair (L, π) , where (1) L is an oriented link in M called *the binding* of the open book; (2) $\pi : M \setminus L \rightarrow S^1$ is a fibration whose fiber, $\pi^{-1}(\theta)$, called a *page*, is the interior of a compact surface $\Sigma_\theta \subset M$ such that $\partial\Sigma_\theta = L$ for all $\theta \in S^1$.

One of the central results about the topology of contact 3-manifolds is Giroux correspondence [9]:

$$\left\{ \begin{array}{l} \text{contact structures } \xi \text{ on } M^3 \\ \text{up to contact isotopy} \end{array} \right\} \xleftrightarrow{1-1} \left\{ \begin{array}{l} \text{open book decompositions } (\Sigma, \phi) \\ \text{of } M^3 \text{ up to positive stabilization} \end{array} \right\}.$$

For example, the standard contact structure $\xi_{std} = \ker(dz + r^2 d\theta)$ on $S^3 = \mathbb{R}^3 \cup \{\infty\}$ corresponds to the open book decomposition (D^2, id) .

We define a braid and the braid index in a general open book setting:

Definition 1.2. Suppose (L, π) is an open book decomposition for a 3-manifold M . A link $K \subset M$ is called a (closed) *braid* if K transversely intersects each page $\Sigma_\theta = \pi^{-1}(\theta)$ of the open book. That is, at each point $p \in K \cap \Sigma_\theta$, we have $T_p \Sigma_\theta \oplus T_p K = T_p M$. The *braid index* of a braid K is the degree of the map π restricted to K . In other words, if a braid K intersects each page in n points, then the braid index of K is n .

Date: November 27, 2010.

2000 *Mathematics Subject Classification.* Primary 57M25, 57M27; Secondary 57M50.

The first author was partially supported by NSF grants DMS-0806492 and DMS-0635607.

Bennequin [2] proved that any transverse link in (S^3, ξ_{std}) can be transversely isotoped to a closed braid in (D^2, id) . Later the second author generalized Bennequin's result into the following:

Theorem 1.3. [13, Theorem 3.2.1] *Suppose (Σ, ϕ) is an open book decomposition for a 3-manifold $M = M_{(\Sigma, \phi)}$. Let $\xi = \xi_{(\Sigma, \phi)}$ be a compatible contact structure. Let K be a transverse link in (M, ξ) . Then K can be transversely isotoped to a braid in (Σ, ϕ) .*

The *self linking (Bennequin) number* is a classical invariant for transverse knots. Bennequin [2] gave a formula of the self linking number for a braid b in (D^2, id) :

$$(1.1) \quad sl(b) = -n + a,$$

where n is the braid index, and a the algebraic crossing number (the exponent sum) of the braid.

The first goal of this paper is to give a combinatorial description for the self linking number of a null-homologous transverse link in the contact lens spaces compatible with (A, D^k) the annulus A open book decomposition with monodromy the k^{th} power of the positive Dehn twist D . By Theorem 1.3, our problem is reduced to searching a self linking formula for a null-homologous braid in the open book decomposition (A, D^k) . Such a braid is given by a product of permutations of points in a local disk on the annulus A and moves of points which turn around the hole of A . We denote by a_σ the algebraic crossing number of the local permutations, and by a_ρ the algebraic rotation number around the hole of A , see Definition 2.5 for precise definitions. With these notations, we extend Bennequin's formula (1.1) into the following:

Theorem 4.1. *Let b be a null-homologous closed braid in (A, D^k) of braid index n . For $k \neq 0$ we have*

$$sl(b) = -n + a_\sigma + a_\rho \left(1 - \frac{a_\rho}{k}\right).$$

When $k = 0$ there exists a canonical Seifert surface Σ_b of b and we have

$$sl(b, \Sigma_b) = -n + a_\sigma.$$

The Seifert surface Σ_b will be constructed in Section 3. The surface is canonical in the sense that the way of construction is similar to that of the standard Seifert surface, or Bennequin surface, of a closed braid in S^3 .

Our second goal is to find a self-linking formula for null-homologous transverse links in a contact Seifert fibered manifold M of signature $(g = 0, k_1, k_2, k_3)$. Let S be a pair of pants (a disk with two holes). Let D_i ($i = 1, 2, 3$) be the positive Dehn twists along the curves parallel to the boundary circles of S . Then M has an open book decomposition $(S, D_1^{k_1} \circ D_2^{k_2} \circ D_3^{k_3})$, and is equipped with a compatible contact structure. A braid in the pants open book is a product of permutations of points in a local disk on S and moves of points which turn around the holes of S . We denote by a_σ the algebraic crossing number of the local permutations and by a_{ρ_i} ($i = 2, 3$) the algebraic winding number around the holes. See Definition 5.4 for precise definitions. We obtain the following formula which also extends (1.1).

Theorem 5.6 *Let b be a null-homologous braid in $(S, D_1^{k_1} \circ D_2^{k_2} \circ D_3^{k_3})$ of braid index n . Suppose k_1, k_2, k_3 are integers with $k_1, k_2, k_3 \geq 0$; $k_1, k_2, k_3 \leq 0$; or $k_1 = 0, k_2 k_3 < 0$. We have:*

$$sl(b, [\Sigma_b]) = -n + a_\sigma + a_{\rho_2}(1 - s_2) + a_{\rho_3}(1 - s_3) - (s_2 + s_3)k_1,$$

where Σ_b is some Seifert surface for b . The constants s_2, s_3 are determined by $a_{\rho_2}, a_{\rho_3}, k_1, k_2$ and k_3 , under the assumption that b is null-homologous, see Definition 5.4.

The organization of the paper is the following:

In Section 2, we fix notations and study properties of the contact lens space $(M_{(A, D^k)}, \xi_k)$.

In Section 3, we construct a Bennequin type Seifert surface \hat{F}_b for a given braid b in (A, D^k) . In general, this \hat{F}_b is an immersed surface and the Bennequin-Eliashberg inequality is not satisfied even for tight cases. We resolve all the singularities and obtain an embedded surface Σ_b . We develop a theory about resolution of singularities of an immersed surface and corresponding changes in characteristic foliations.

In Section 4, we prove Theorem 4.1, an explicit formula of the self linking number relative to Σ_b , which extends Bennequin's formula (1.1). As the self linking number is defined to be the euler number of the contact 2-plane bundle relative to the surface framing, we measure the difference between the immersed \hat{F}_b -framing and the embedded Σ_b -framing. We also study the behavior of our self linking number under a braid stabilization. Corollary 4.5 states that our self linking number is invariant under a positive stabilization and changes by 2 under a negative stabilization, which extends Bennequin's result for braids in (S^3, ξ_{std}) .

In Section 5, we apply our surface construction method to some class of contact Seifert fibered manifolds and prove Theorem 5.6.

Acknowledgements. The authors would like to thank John Etnyre for numerous useful comments and sharing his ideas, especially those on Corollary 3.9, and Matthew Hedden for helpful comments on Section 4. They also thank the referee for carefully examining the paper and providing constructive comments. K.K. thanks Tim Cochran and Walter Neumann for stimulus conversations.

2. PRELIMINARIES

Let $A = S^1 \times I$ be an annulus and D_α the positive Dehn twist about the core circle $\alpha = S^1 \times \{\frac{1}{2}\}$. For simplicity, we denote D_α by D .

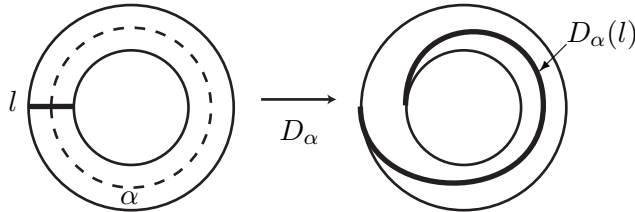


FIGURE 1. A positive Dehn twist D_α about α .

We study an abstract open book decomposition (A, D^k) .

Claim 2.1. *The corresponding manifold $M_{(A, D^k)}$ to (A, D^k) is:*

$$M_{(A, D^k)} = \begin{cases} L(k, k-1) & \text{if } k > 0, \\ S^1 \times S^2 & \text{if } k = 0, \\ L(|k|, 1) & \text{if } k < 0. \end{cases}$$

Proof. Let $D_\circ \simeq D^2$ be a disk and $\gamma := \partial D_\circ$. Recall that (D_\circ, id) is a planar open book decomposition for (S^3, ξ_{std}) . Let $D_\mu \subset D_\circ$ be a disc with boundary μ . The core of the solid torus $D_\mu \times S^1 \subset S^3$ is the unknot, U . The meridian of the torus $T_\mu = \partial(D_\mu \times S^1)$ is μ . Pick a point $p \in \mu$, and define a longitude λ of T_μ as $\lambda = \{p\} \times S^1$. Remove $D_\mu \times S^1$ from S^3 , and attach a new solid torus by identifying its meridian m with λ and its longitude l with $-\mu$. This is the 0-surgery along the unknot U . The resulting manifold is $S^1 \times S^2$. In this way we get an open book decomposition (A, id_A) for $S^1 \times S^2$, whose page A is the union of the annulus $D_\circ \setminus D_\mu$, shaded in Figure 2-(1), and the annulus bounded by $-l$ and the core γ' of the solid torus, sketched in Figure 2-(2).

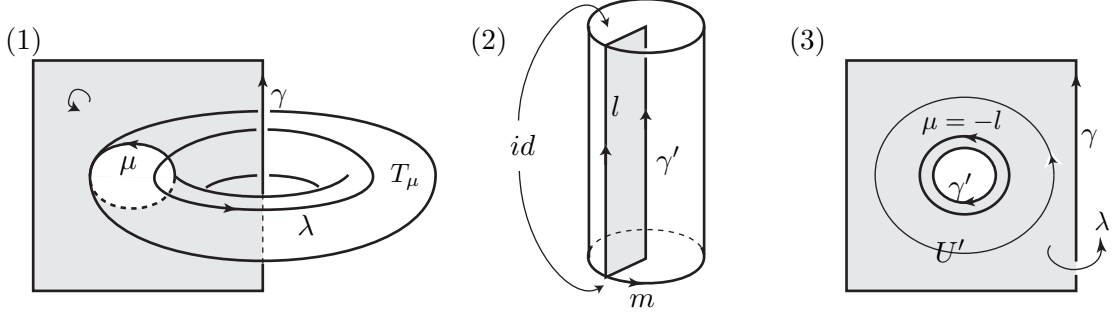


FIGURE 2. (1) Removing a solid torus $D_\mu \times S^1$ from S^3 . (2) The attaching solid torus. (3) The page annulus A .

The Dehn twist D^k about the core $U' \subset (D_\circ \setminus D_\mu) \subset A$, sketched in Figure 2-(3), of the page annulus A is equivalent to applying $(\frac{1}{-k})$ -surgery along the unknot U' . The link $(U \cup U') \subset S^3$ is the positive Hopf link. By the slam-dunk operation, the surgery description is reduced to the k -surgery along U , which represents $L(k, -1) = L(k, k-1)$ when $k > 0$ and $L(|k|, 1)$ when $k < 0$. \square

Let $(M_{(A, D^k)}, \xi_k)$ be the contact manifold corresponds to the open book (A, D^k) .

Claim 2.2. *The contact manifold $(M_{(A, D^k)}, \xi_k)$ is overtwisted if and only if $k < 0$. When $k \geq 0$, this ξ_k is the unique tight contact structure for $L(k, k-1)$.*

Proof. If $k < 0$, Goodman's criterion for overtwistedness [10, Theorem 1.2] implies that ξ_k is overtwisted.

When $k = 0$, according to [6, proof of Lemma 3.2] of Etnyre-Honda, the open book is a boundary of a positive Lefschetz fibration on a 4-manifold X , so that $(S^1 \times S^2, \xi_0)$ is Stein filled by X , hence tight. Moreover, ξ_0 is the unique tight contact structure on $S^2 \times S^1$ due to Eliashberg [3].

When $k > 0$, the monodromy is a product of positive Dehn twists. Etnyre-Honda's [6, Lemma 3.2] guarantees that the contact structure compatible with such an open book is

Stein fillable, hence tight. The uniqueness for $k > 0$ follows from Honda's classification of tight contact structures for lens spaces [11]. More precisely, we have

$$-\frac{k}{k-1} = -2 - \frac{1}{-2 - \frac{1}{-2 - \dots - \frac{1}{-2}}}$$

repeating $(k-1)$ -times

and $|(-2+1)(-2+1)\cdots(-2+1)| = 1$, thus the manifold has the unique tight contact structure. \square

We fix notations. See Figure 3. Suppose we have a null-homologous closed braid b of braid index n in the open book (A, D^k) . Let $\gamma \cup \gamma' = \partial A$ whose orientations are induced by that of A . Let A_θ ($\theta \in [0, 1]$) denote the page $A \times \{\theta\} \subset M_{(A, D^k)}$. Under the identification $A = S^1 \times [0, 1]$, we set $\alpha = S^1 \times \{\frac{1}{2}\}$. Let β be a circle between α and γ which is oriented clockwise.

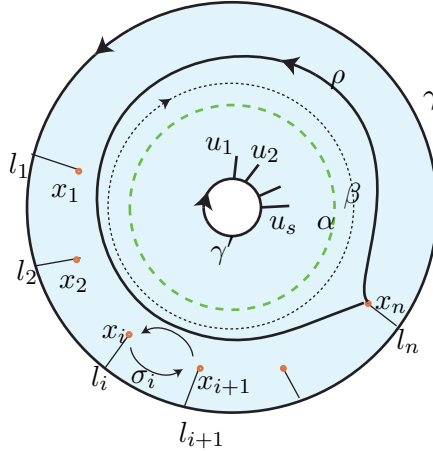


FIGURE 3.

Assumption 2.3. Choose points x_1, \dots, x_n sitting between γ and α . By braid isotopy, which preserves the transverse knot class (Theorem 2.8-(2)), we may assume that:

$$b \cap A_0 = \{x_1, \dots, x_n\}.$$

Let σ_i ($i = 1, \dots, n-1$) be the generators of Artin's braid group B_n satisfying $\sigma_i \sigma_{i+1} \sigma_i = \sigma_{i+1} \sigma_i \sigma_{i+1}$ and $\sigma_i \sigma_j = \sigma_j \sigma_i$ for $|i-j| \geq 2$. Geometrically, σ_i acts by switching the marked points x_i and x_{i+1} counterclockwise. The circle β will appear in Section 3.1. Let ρ be a braid element which moves x_n once around the annulus in the indicated direction.

Proposition 2.4. An n -strand braid b in (A, D^k) has a braid word in $\{\sigma_1, \dots, \sigma_{n-1}, \rho\}$.

Proof. Let $D_\bullet \subset D_\circ$ be concentric disks of center o . Identify the annulus A with $D_\circ \setminus D_\bullet$ and $\partial D_\bullet = -\gamma'$, $\partial D_\circ = \gamma$. Consider the union $\tilde{b} := b \cup (\{o\} \times [0, 1]) \subset D_\circ \times [0, 1]$, which we identify with an $(n+1)$ -strand braid in Artin's braid group B_{n+1} . Let $p : D_\circ \times [0, 1] \rightarrow D_\circ$

be the projection onto the first factor. Up to homotopy, we can think that $p(\{o\} \times [0, 1])$ is a (non-simple) closed curve in $D_o \setminus \{x_1, \dots, x_n\}$. Denote its homotopy class by

$$b_\bullet := [p(\{o\} \times [0, 1])] \in \pi_1(D_o \setminus \{x_1, \dots, x_n\}, o).$$

Let ρ_1, \dots, ρ_n be generators of $\pi_1(D_o \setminus \{x_1, \dots, x_n\}, o)$ as in Figure 4-(1). The transition

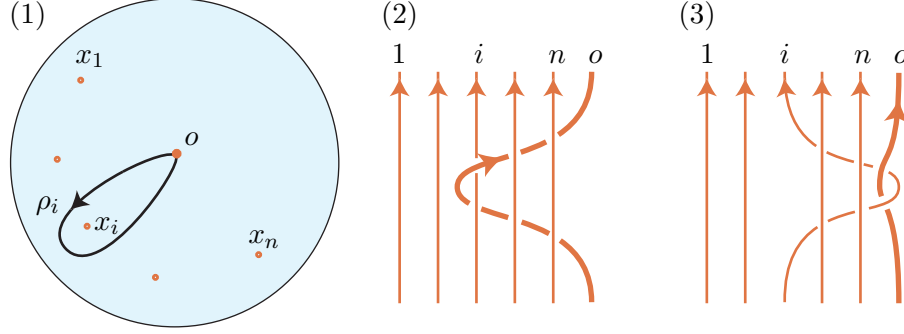


FIGURE 4.

from Figure 4-(2) to (3) shows:

$$\begin{aligned} \rho_i &= \sigma_i^{-1} \cdots \sigma_{n-1}^{-1} \sigma_n^2 \sigma_{n-1} \cdots \sigma_i, \quad (i = 1, \dots, n-1), \\ \rho_n &= \sigma_n^2. \end{aligned}$$

Since our $\rho = \rho_n$ is equal to σ_n^2 in the braid group B_{n+1} , the braid \tilde{b} can be written in letters $\{\sigma_1, \dots, \sigma_{n-1}, \rho\}$. Since $b \subset \tilde{b}$, the statement of the proposition follows. \square

Definition 2.5. Let $a_\sigma \in \mathbb{Z}$ (resp. $a_\rho \in \mathbb{Z}$) be the exponent sum of $\sigma_1, \dots, \sigma_{n-1}$'s (resp. ρ) in the braid word of b .

Proposition 2.6. *If $k > 0$ (resp. $k < 0$), we may assume that $a_\rho \geq 0$ (resp. $a_\rho \leq 0$).*

To prove Proposition 2.6, we first define braid stabilization and recall its properties.

Definition 2.7. Let b be a closed braid in an open book (Σ, ϕ) . Suppose that $\lambda \subset \partial\Sigma$ is one of the bindings of the open book and $p \in (\Sigma_\theta \cap b)$ is a point, see Figure 5. Join p and a point on λ by an arc $a \subset (\Sigma_\theta \setminus b)$. A *positive (negative) stabilization* of b about λ along a is pulling a small neighborhood of p of the braid, then adding a positive (negative) kink about λ in a neighborhood of a .

The second author proved Markov theorem in a general open book setting:

Theorem 2.8. [13, Theorem 4.1.3 and 4.1.4]

- (1) *Two closed braids K_1 and K_2 in an open book decomposition have the same topological type if and only if they are related by braid isotopy, positive and negative braid stabilizations.*
- (2) *The above K_1, K_2 are transversely isotopic if and only if they are related by braid isotopy and positive braid stabilizations.*



FIGURE 5. Positive braid stabilization along a .

Proof of Proposition 2.6. Suppose b is an n -strand braid. Recall that (A, D^k) has two binding components, γ and γ' . Let a be an arc joining x_n and γ' and intersecting α at a point as sketched in Figure 6. Pick a small line segment of the n^{th} strand in

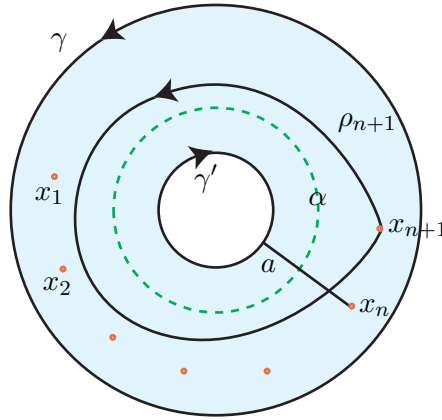


FIGURE 6. Definitions of a, x_{n+1} and ρ_{n+1} .

$A \times (1 - \epsilon, 1)$, near the top page $A_{\theta=1}$ of the open book, and positively stabilize it along a . As a consequence, it gains a new braid strand, which we call ν , lying in a small tubular neighborhood of γ' , see Figure 7-(1). Put a point $x_{n+1} \subset A$ on the right side of x_n between γ and define ρ_{n+1} a braid generator as in Figure 6. Move ν by a braid isotopy supported in $A \times (1 - \epsilon, 1 + \epsilon)$ so that ν intersects the page $A_0 = A_1$ at x_{n+1} . This isotopy introduces $(\rho_{n+1})^k$ in $A \times (0, \epsilon)$ as a consequence of the monodromy D^k . Compare Figure 7-(1) and (2).

We observe that in a stabilized braid, ρ_{n+1} plays the role of the old $\rho = \rho_n$ and as Figure 7-(3) shows, they are related by:

$$(2.1) \quad \rho_n = \sigma_n \rho_{n+1} \sigma_n.$$

Thus a positive stabilization about γ' takes a word b to $(\rho_{n+1})^k \tilde{b} \sigma_n$, where \tilde{b} is obtained from b replacing each ρ with $\sigma_n \rho_{n+1} \sigma_n$. The data change in the following way:

$$n \rightarrow n + 1, \quad a_\sigma \rightarrow a_\sigma + 1 + 2a_\rho, \quad a_\rho \rightarrow a_\rho + k.$$

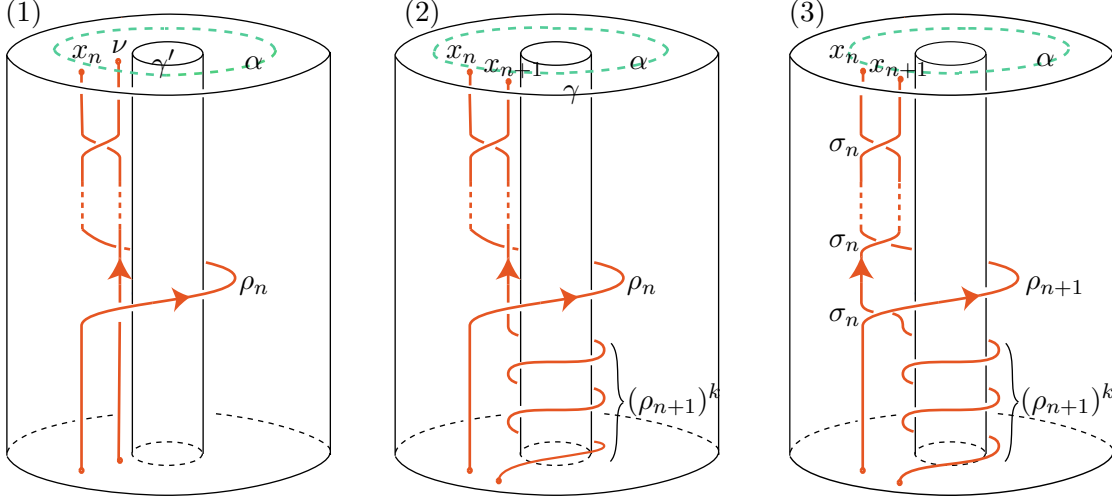


FIGURE 7. (1) Positive stabilization about the binding γ' . (2) Transversely isotope ν near γ' to x_{n+1} near γ . This introduces k additional ρ_{n+1} 's. (3) ρ_n and ρ_{n+1} are related by $\rho_n = \sigma_n \rho_{n+1} \sigma_n$.

Theorem 2.8-(2) tells that a positive stabilization preserves the transverse knot type, so if $k > 0$ (resp. $k < 0$) we may assume that $a_\rho \geq 0$ (resp. $a_\rho \leq 0$). \square

The next corollary introduces a number s :

Corollary 2.9. *If $k \neq 0$ there exists a non-negative integer s such that $a_\rho = sk$. If $k = 0$ then $a_\rho = 0$.*

Proof. In the homology group $H_1(M_{(A,D^k)}, \mathbb{Z})$, we have $[b] + a_\rho[\beta] = 0$. Since the braid b is null-homologous $a_\rho[\beta] = [b] = 0$. The meridian μ introduced in the proof of Claim 2.1 is a generator of $H_1(M_{(A,D^k)}, \mathbb{Z}) = \mathbb{Z}/k\mathbb{Z}$. Since $a_\rho[-\mu] = a_\rho[\beta] = 0$ we have $a_\rho \equiv 0 \pmod{k}$, implying the existence of $s \in \mathbb{Z}$ with $a_\rho = sk$ for $k \neq 0$. Proposition 2.6 guarantees that we may assume $s \geq 0$. When $k = 0$, we have $a_\rho = 0$. \square

3. CONSTRUCTION OF SEIFERT SURFACE Σ_b

The goal of this section is to construct a Seifert surface Σ_b for a null-homologous braid b whose braid word is written in $\{\sigma_1, \dots, \sigma_{n-1}, \rho\}$. (By abuse of notation, we use b for both the closed braid and its braid word.) We first construct a surface F_b and change it to \tilde{F}_b . We further deform $\tilde{F}_b \rightarrow \check{F}_b \rightarrow \hat{F}_b$ and finally obtain Σ_b .

3.1. Construction of the surface F_b . Let $l_i \subset A$ be a line segment perpendicular to γ having x_i as one of its endpoints and with the other end on γ , see Figure 3. Since l_i is disjoint from the Dehn twist curve α , in the resulting manifold, $M_{(A,D^k)}$, the arc l_i swipes a disk $\delta_i := (l_i \times [0, 1]) / \sim$. See Figure 8. The center of δ_i is $l_i \cap \gamma$. We orient δ_i so that the binding γ is positively transverse to δ_i .

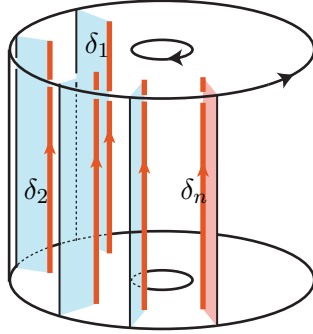


FIGURE 8. Oriented disks $\delta_1, \dots, \delta_n$. Positive (negative) side is light blue (dark pink).

Suppose the braid word for b has length m . If the j^{th} ($1 \leq j \leq m$) letter is σ_i (resp. σ_i^{-1}) then we join the disks δ_i and δ_{i+1} by a positively (resp. negatively) twisted band embedded in the set of pages $\{A_\theta \mid \frac{j-1}{m} < \theta < \frac{j}{m}\}$. See Figure 9-(1).

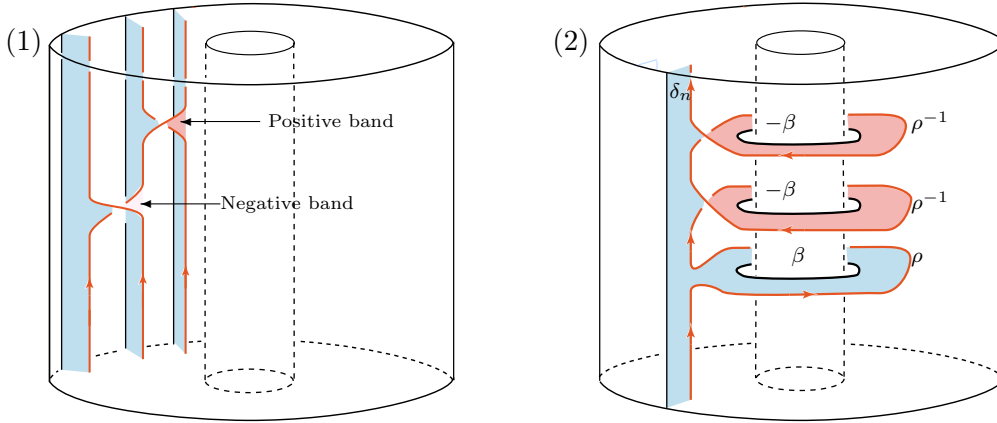
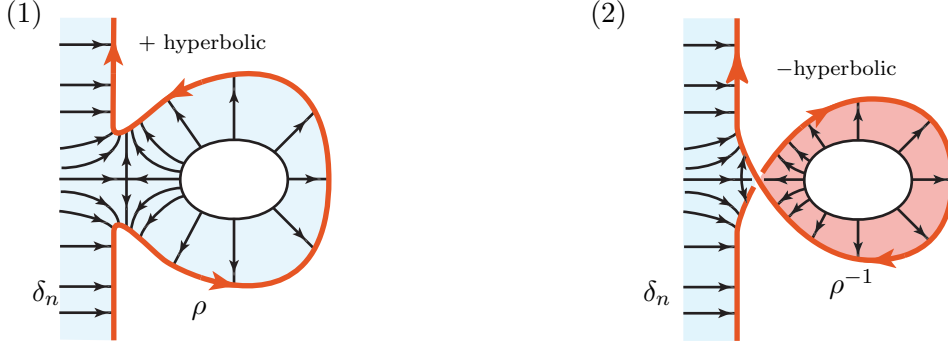


FIGURE 9. Construction of F_b . (1) Twisted bands. (2) \mathfrak{A} -annuli.

If the j^{th} letter is ρ (resp. ρ^{-1}), then we attach to the disk δ_n an annulus embedded in $\{A_\theta \mid \frac{j-1}{m} < \theta < \frac{j}{m}\}$. We call such an annulus an \mathfrak{A} -annulus. See Figure 9-(2). Let $\beta \subset A$ be an oriented circle between circles α and γ as sketched in Figure 3. One of the boundaries of each \mathfrak{A} -annulus represents ρ (resp. ρ^{-1}) and becomes part of the braid b . The other boundary, which we denote by β_j (resp. $-\beta_j$), is in $\beta \times (\frac{j-1}{m}, \frac{j}{m})$.

We call the resulting surface F_b .

By [8, Proposition 4.6.11], we may assume that the characteristic foliation of our surface is of Morse-Smale type. Each disk δ_i has a positive elliptic point. A positive (negative) band between the δ -disks contributes one positive (negative) hyperbolic point. The foliation on the disk δ_n together with an attached \mathfrak{A} -annulus has a positive (resp. negative) hyperbolic singularity as sketched in Figure 10-(1) (resp. (2)) if the corresponding braid word is ρ (resp. ρ^{-1}).

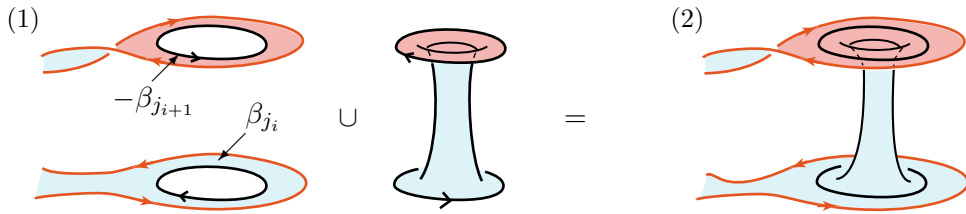
FIGURE 10. Characteristic foliations of \mathfrak{A} -annulus for (1) ρ and (2) ρ^{-1} .

3.2. Construction of the surface \tilde{F}_b . In Section 3.1, we have constructed an embedded oriented surface F_b whose boundary consists of the braid b and copies of $\pm\beta$'s. Let $a_\sigma \in \mathbb{Z}$ (resp. $a_\rho \in \mathbb{Z}$) be the exponent sum of $\sigma_1, \dots, \sigma_{n-1}$'s (resp. ρ 's) in the braid word for b . Let r be the number of ρ^{\pm} 's appearing in the braid word for b of length m (i.e., $0 \leq r \leq m$). Then there exist $1 \leq j_1 < \dots < j_r \leq m$ and $\epsilon_i = \pm 1$ with $\epsilon_1 + \epsilon_2 + \dots + \epsilon_r = a_\rho$ such that

$$\partial F_b = b \cup \epsilon_1 \beta_{j_1} \cup \epsilon_2 \beta_{j_2} \cup \dots \cup \epsilon_r \beta_{j_r}.$$

Proposition 3.1. *By attaching vertical annuli to pairs of β and $-\beta$ circles as described in Figure 11, we can construct an embedded oriented surface, which we call \tilde{F}_b , whose boundary consists of*

$$(3.1) \quad \partial \tilde{F}_b = \begin{cases} b \text{ and } a_\rho \text{ copies of } \beta, & \text{if } k > 0, \\ b, & \text{if } k = 0, \\ b \text{ and } -a_\rho \text{ copies of } -\beta, & \text{if } k < 0. \end{cases}$$

FIGURE 11. Attaching a vertical annulus to \mathfrak{A} -annuli.

Proof. Suppose that $\partial F_b = b \cup \epsilon_1 \beta_{j_1} \cup \epsilon_2 \beta_{j_2} \cup \dots \cup \epsilon_r \beta_{j_r}$ and $\epsilon_1 + \epsilon_2 + \dots + \epsilon_r = a_\rho$.

If $\epsilon_1 = \epsilon_2 = \dots = \epsilon_r$ (ρ and ρ^{-1} do not coexist in the braid word for b), then take $\tilde{F}_b = F_b$.

Else, let $1 \leq i \leq r-1$ be the smallest index for which $\epsilon_i \neq \epsilon_{i+1}$. We attach a “vertical” annulus to $(\epsilon_i \beta_{j_i}) \cup (\epsilon_{i+1} \beta_{j_{i+1}})$ as sketched in Figure 11. The boundary of the newly obtained surface (call this surface $F_{b,1}$) contains two less $\pm\beta$ -curves:

$$\partial F_{b,1} = b \cup \epsilon_1 \beta_{j_1} \cup \dots \cup \epsilon_{i-1} \beta_{j_{i-1}} \cup \epsilon_{i+2} \beta_{j_{i+2}} \cup \dots \cup \epsilon_r \beta_{j_r}$$

but it preserves the sum: $\epsilon_1 + \cdots + \epsilon_{i-1} + \epsilon_{i+2} + \cdots + \epsilon_r = a_\rho$.

Renumber the the boundary components,

$$\partial F_{b,1} = b \cup \epsilon_1 \beta_{j_1} \cup \epsilon_2 \beta_{j_2} \cup \cdots \cup \epsilon_{r-2} \beta_{j_{r-2}}$$

then repeat the procedure for $F_{b,1}$. If $i-1$ is the smallest index for which $\epsilon_{i-1} \neq \epsilon_i$, then attach the annulus by nesting it inside the one previously attached. See the right sketch in Figure 12. After at most $\lceil \frac{r}{2} \rceil$ such attachments of annuli, all the ϵ_i 's have the same

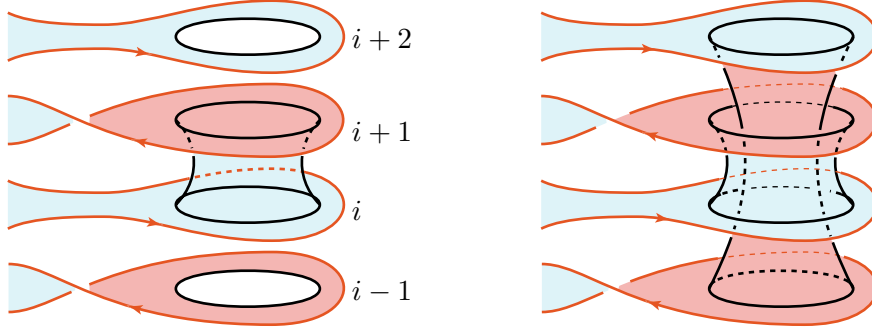


FIGURE 12. Nested vertical annuli

sign, and we get the desired surface \tilde{F}_b . By Proposition 2.6 and Corollary 2.9 we have the equality (3.1). \square

3.3. Construction of the immersed surface \tilde{F}_b . We have constructed a surface \tilde{F}_b satisfying the boundary condition (3.1). In particular, when $k = 0$ we have already obtained an embedded surface \tilde{F}_b whose boundary is b . Define $\Sigma_b := \tilde{F}_b$.

When $k \neq 0$, we construct an immersed surface \check{F}_b from \tilde{F}_b , by attaching disks about the binding γ' .

Assume that $k > 0$. Proposition 2.6 justifies assuming $a_\rho \geq 0$. Let $\mathfrak{A}_1, \dots, \mathfrak{A}_{a_\rho} \subset \tilde{F}_b$ be the \mathfrak{A} -annuli whose boundaries contribute to the a_ρ copies of β -circles as in Proposition 3.1. Recall the number $s = \frac{a_\rho}{k} \geq 0$ defined in Corollary 2.9. Let $u_1, \dots, u_s \subset A$ be arcs, see Figure 3, disjoint from the Dehn twist circle α , such that one end of each u_i sits on the binding γ' . Let $\omega_1, \dots, \omega_s$ be disks, called ω -disks, obtained by swiping u_1, \dots, u_s in the open book (A, D^k) so that the center of ω_i is pierced by γ' . For each $i = 1, \dots, s$, connect ω_i smoothly with annuli $\mathfrak{A}_i, \mathfrak{A}_{s+i}, \mathfrak{A}_{2s+i}, \dots, \mathfrak{A}_{(k-1)s+i}$ by k copies of the twisted band as in Figure 13-(1). When $k < 0$, attach twisted bands as in Figure 13-(2). We have obtained an immersed surface, which we denote by \check{F}_b , see Figure 14.

Lemma 3.2. *Regardless of the sign of k , all the singularities for the characteristic foliation of the attached bands and the ω -disks are positive elliptic.*

Remark 3.3. The surface \check{F}_b has s additional positive elliptic points compared to \tilde{F}_b .

Proof. By definition of ω -disk, its characteristic foliation has a single singularity at its center and it is of elliptic type (Figure 13). The orientation of ω -disk is induced from that of the \mathfrak{A} -annuli so that the sign of the elliptic point is positive regardless of the sign of k .

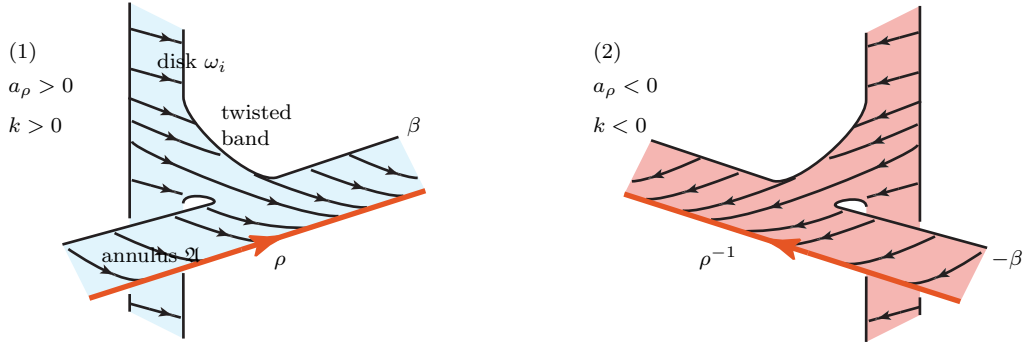


FIGURE 13. An ω -disk and an \mathfrak{A} -annulus joined by a twisted band.

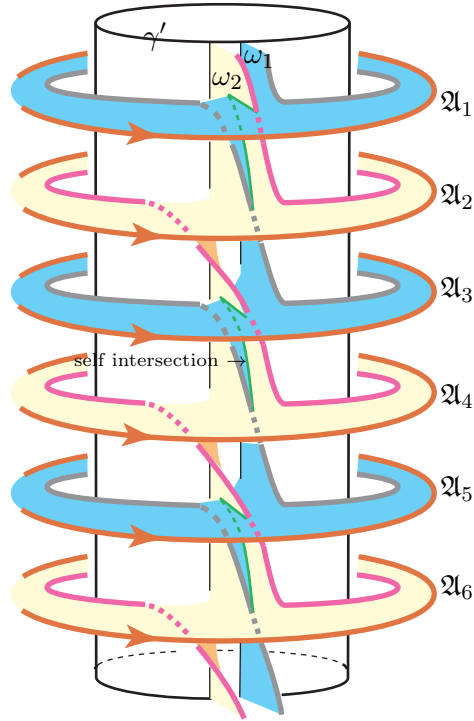


FIGURE 14. A part of immersed surface \tilde{F}_b for $k = 3, a_\rho = 6, s = 2$. Two ω -disks and six \mathfrak{A} -annuli joined by twisted bands. Self intersections are marked by thin green curves.

In the following, we show that there are no hyperbolic points on the twisted band. See Figure 15. Parameterize the twisted band as $[0, 1] \times [-1, 1]$. Attach the side $\{0\} \times [-1, 1]$ of the band to the ω -disk and $\{1\} \times [-1, 1]$ to the β -circle so that the (dashed) line segment $[0, 1] \times \{\frac{1}{2}\}$ sit on one page of the open book. We make the resulting surface smooth near the two attaching sides of the band. Take points on the twisted band

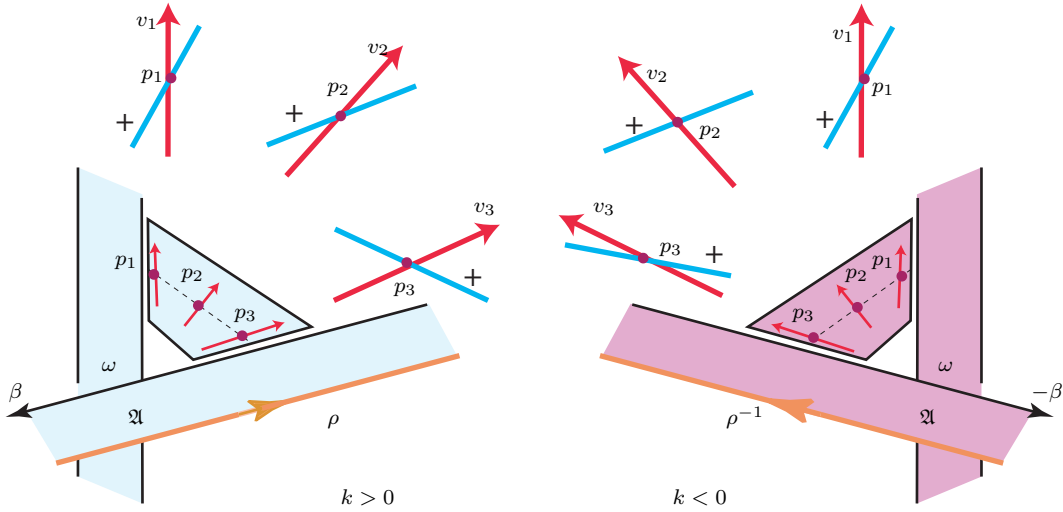


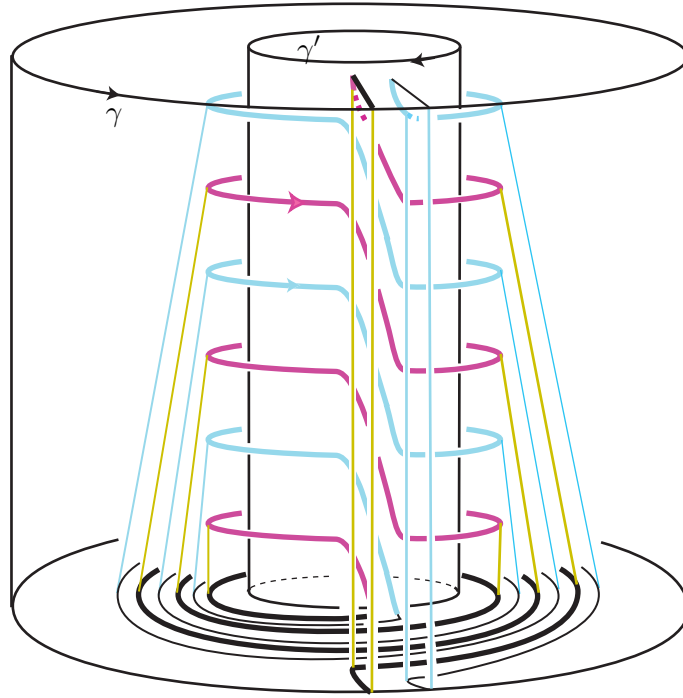
FIGURE 15. Proof of Lemma 3.2

$p_1 = (0, \frac{1}{2})$, $p_2 = (\frac{1}{2}, \frac{1}{2})$, and $p_3 = (1, \frac{1}{2})$. Let v_i be a tangent vector (red arrow) of the band at p_i that is perpendicular to the dashed line $[0, 1] \times \{\frac{1}{2}\}$.

When $k > 0$, with respect to the page of the open book, v_1 is vertical, v_2 is slanted 45° , and v_3 is slanted ϵ -degree ($0 < \epsilon < 45$) because the braid b transversely intersects all the pages of the open book positively. Next we look at contact planes ξ_{p_i} (light blue line segment) at p_i . In Figure 15, the positive side of a contact plane is marked “+”. At each point of the bindings γ, γ' , we may assume that the contact plane is positively perpendicular to the binding. Between the bindings, the contact planes rotate 180° counter clockwise along the radial lines. Since p_1 is close to the binding γ' , for some $\epsilon_1 > 0$, ξ_{p_1} is slanted $(90 - \epsilon_1)$ -degree with respect to the page of the open book. While, ξ_{p_3} is slanted $(-\epsilon_3)$ -degree for some $\epsilon_3 > 0$ since p_3 is on the circle β which is between α and γ (Figure 3). At any point between p_1 and p_3 on the dashed line, the tangent plane is slanted more than the contact plane. It means that they never coincide. Since the band is a small neighborhood of the dashed line, contact planes are never tangent to the band, hence there are no singularities in the characteristic foliation on the twisted band.

When $k < 0$, at p_3 , the tangent vector v_3 is slanted $(180 - \epsilon)$ -degree and the contact plane ξ_{p_3} is slanted $(-\epsilon_3)$ -degree. Braid b is a transverse link so it intersects contact planes positively. Considering that p_3 is close to the braid (orange arc), v_3 intersects ξ_{p_3} positively, i.e., $\epsilon > \epsilon_3$. Therefore, the tangent planes and the contact planes never coincide along the dashed line from p_1 to p_3 , hence there are no singularities in the characteristic foliation on the twisted band. \square

3.4. Construction of the immersed surface \hat{F}_b . Let τ be a closed braid in (A, D^k) of braid index = 1. The immersed surface \check{F}_b constructed in Section 3.3 has boundary $[b] + s[\tau + k\beta]$ in $H_1(M_{(A, D^k)}, \mathbb{Z})$. Each closed curve representing $-\tau + k\beta$ bounds a disk about the binding γ . We call it a \mathcal{D} -disk, see Figure 16. There, the spirals in the bottom annulus page are identified, via the Dehn twist D^k , with the straight line

FIGURE 16. \mathcal{D} -disks

segments in the top annulus page. There are s -copies of \mathcal{D} -disk and they are disjoint from each other. Since \mathcal{D} -disks are nearly ‘vertical’ as in Figure 16, the tangent planes and the contact planes, which rotate 180° counter clockwise along the radial lines from γ to γ' , intersect transversely. This means that the characteristic foliation of each \mathcal{D} -disk has a single singularity, which occurs at the intersection point with γ and whose type is elliptic. The orientations of the \mathcal{D} -disks are compatible with those of the boundaries so that the \mathcal{D} -disks and γ intersect negatively. Therefore the signs of the elliptic points are negative.

Definition 3.4. We construct an immersed surface \hat{F}_b by glueing the \mathcal{D} -disks and \check{F}_b along the s copies of the $\tau + k\beta$ curve.

Remark 3.5. This \hat{F}_b has s additional negative elliptic singularities given by the \mathcal{D} -disks compared to the surface \check{F}_b .

3.5. Resolution of singularities. We start this section by defining three types of intersection of surfaces; branch, clasp, and ribbon, then study resolution of self-intersections.

Definition 3.6. Let Σ be an immersed oriented surfaces with $\partial\Sigma = K$ given by the immersion $i : \tilde{\Sigma} \rightarrow \Sigma$. Let $l \subset \Sigma$ be a simple arc where Σ intersects itself, and denote by p and q the endpoints of l .

- If p is sitting on K , and q is a branch point of a neighborhood Riemann surface, see Figure 17-(1), then we call l a *branch* intersection.

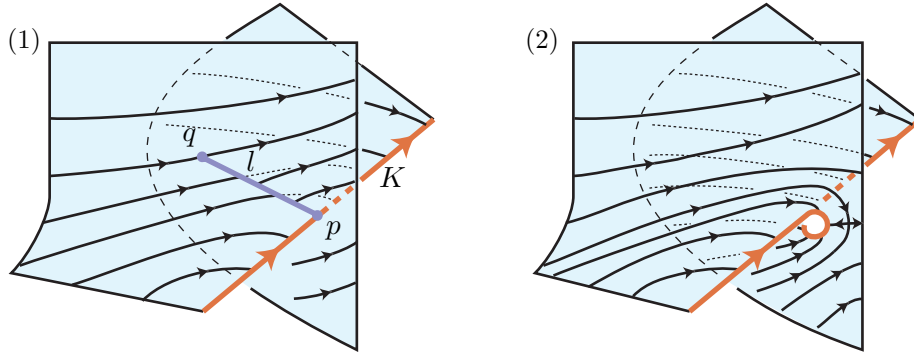


FIGURE 17. (1) A negative branch intersection l , and (2) its resolution.

Next assume that the preimage of l , $i^{-1}(l) \subset \tilde{\Sigma}$, consists of two arcs, say \tilde{l}_1, \tilde{l}_2 . Denote the end points of \tilde{l}_i by \tilde{p}_i and \tilde{q}_i for $i = 1, 2$.

- If $\tilde{p}_1, \tilde{q}_2 \in \partial\Sigma$ and $\tilde{p}_2, \tilde{q}_1 \in \text{Int}(\tilde{\Sigma})$ then we call the intersection a *clasp* intersection. A local picture of l is the left sketch of Figure 18.

- If $\tilde{p}_1, \tilde{q}_1 \in \partial\Sigma$ and $\tilde{p}_2, \tilde{q}_2 \in \text{Int}(\tilde{\Sigma})$ then we call the intersection a *ribbon* intersection. See the right sketch of Figure 18.

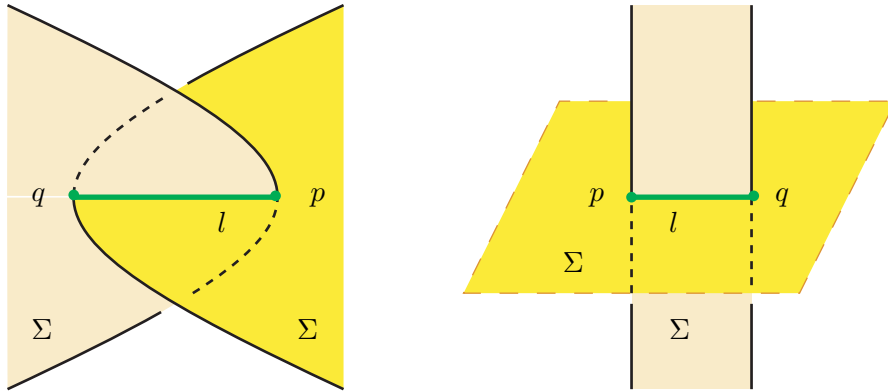


FIGURE 18. (Left) A clasp intersection. (Right) A ribbon intersection.

Example 3.7. See Figure 19. The immersed surface, \hat{F}_b , has:

- $|a_\rho|$ branches formed by \mathfrak{A} -annuli and \mathcal{D} -disks.
- $|k|\binom{s}{2} = \frac{1}{2}|a_\rho|(s-1)$ clasp intersections when $s > 1$. Recall that \hat{F}_b is obtained by attaching s copies of \mathcal{D} -disk about the binding γ . Each pair among these s disks interacts as in Figure 19 giving rise to $|k|$ clasp intersections. When $s = 1, 0$, there are no clasps.
- several ribbon intersections of \mathcal{D} -disks and the (nested) vertical annuli of Figure 11.

In Section 3.6, we resolve these self-intersections to obtain an embedded surface Σ_b .

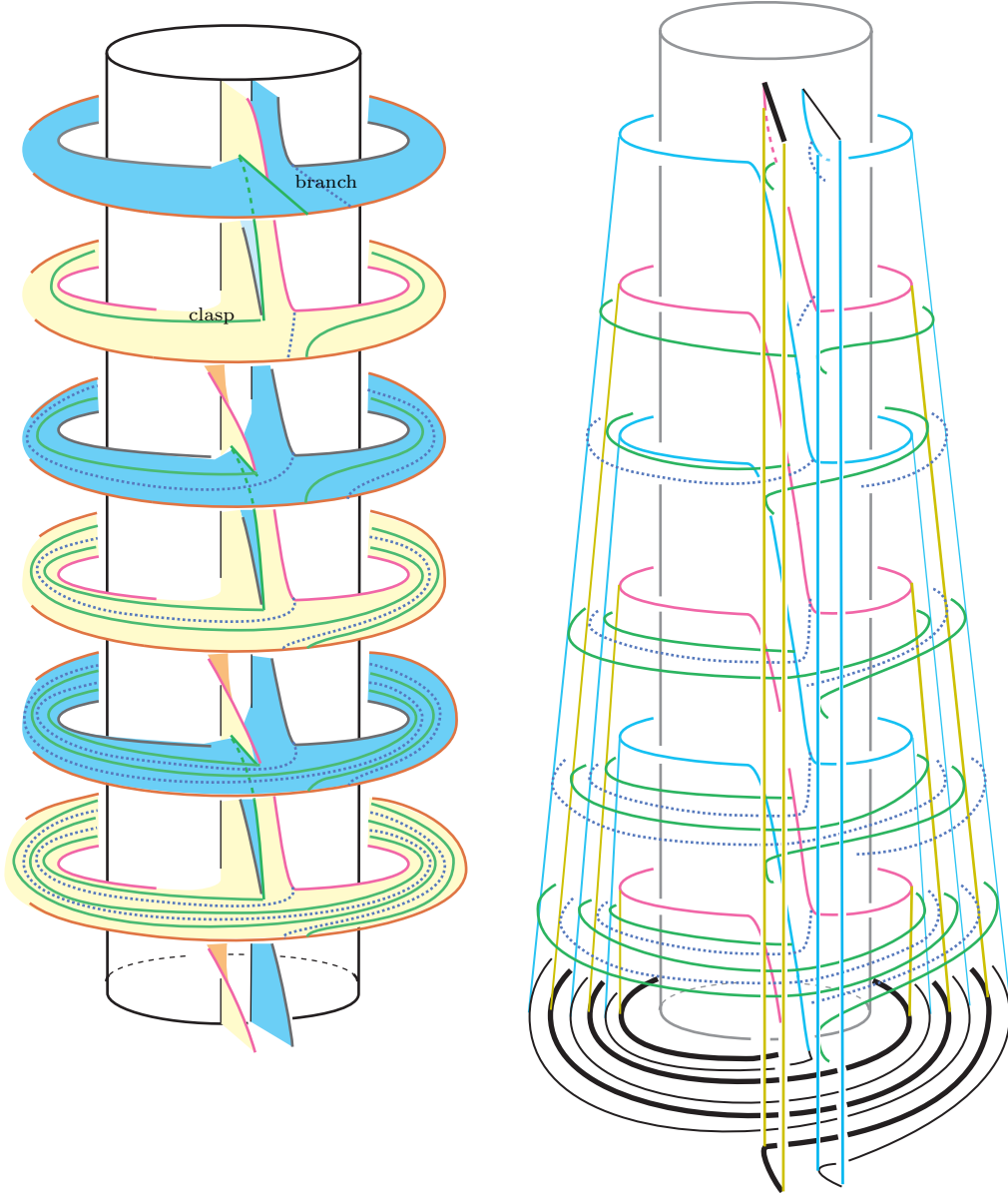


FIGURE 19. Clasp (green) and branch (dashed purple) intersections on \hat{F}_b .

In the following, we assume that K is a transverse knot in a contact manifold (M, ξ) and Σ an immersed oriented surface with $\partial\Sigma = K$. Also, we assume that (i) the self-intersection set of Σ consists of ribbon, clasp, or branch intersections; (ii) the characteristic foliation \mathcal{F}_Σ is of Morse-Smale type.

Let $l \subset \Sigma$ be a self-intersection arc. Near a point $x \in \text{Int}(l)$, Σ intersects itself transversely as in Figure 20-(1). Let $F_i \subset \Sigma$ ($i = 1, 2, 3, 4$) be surfaces meeting at l . The orientation of F_i is induced from that of Σ . Resolve the singularity l by cutting Σ out

along l and re-gluing F_1, F_2 along l and F_3, F_4 along l so that the orientations of the surfaces agree. See Figure 20-(2). Call the new surface Σ' .

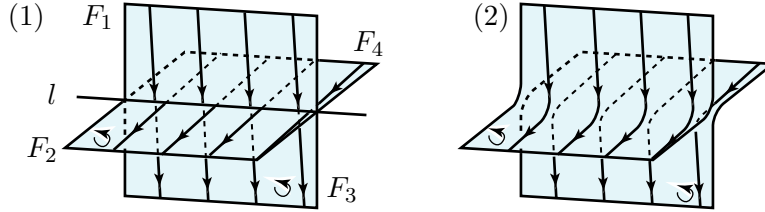


FIGURE 20. (1) Immersed surface Σ . (2) New surface Σ' after resolution of singularity l .

We orient the leaves of the characteristic foliation following [12, page 80]: For $p \in \Sigma$ a nonsingular point of a leaf L of the foliation, let $\vec{n} \in T_p\Sigma$ be a positive normal vector to ξ_p . We choose a vector $\vec{v} \in T_pL$ so that (\vec{v}, \vec{n}) is a positive basis for $T_p\Sigma$. This vector field \vec{v} determines the orientation of the characteristic foliation.

We observe that if both \mathcal{F}_{F_1} and \mathcal{F}_{F_2} transversely intersect the line l (Figure 20-(1)), then the orientations of \mathcal{F}_{F_1} and \mathcal{F}_{F_2} agree at l . Hence, after the cut and glue operation, the new characteristic foliation $\mathcal{F}_{\Sigma'}$ is obtained by smoothly connecting the old \mathcal{F}_{F_1} and \mathcal{F}_{F_2} , and also \mathcal{F}_{F_3} and \mathcal{F}_{F_4} . See Figure 20-(2).

Near the endpoints of l , this resolution creates new hyperbolic points and $\mathcal{F}_{\Sigma'}$ can be made into Morse-Smale type. See Figure 17-(2) and Figure 21-(2). The signs of the new

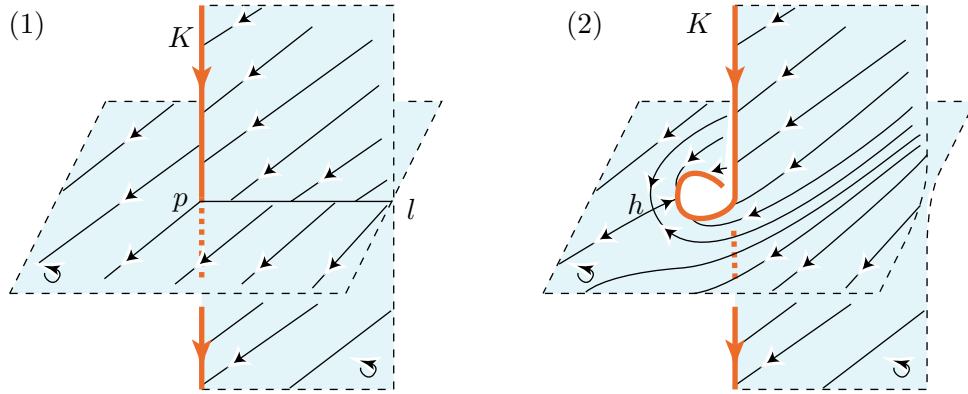


FIGURE 21. (1) A negative intersection p . (2) Creation of a negative hyperbolic singularity h by resolving singular arc l .

hyperbolic points are determined in the following way:

Proposition 3.8. *Suppose that $p \in \partial l \cap K$ and both \mathcal{F}_{F_1} and \mathcal{F}_{F_2} are transversely intersecting with l . If p is a positive (negative) transverse intersection of K and Σ , then the new hyperbolic point has positive (negative) sign.*

Proof. Assume that p is a negative intersection, as depicted in Figure 21-(1). We introduce an (x, y, z) -coordinate system for a small neighborhood N of p : Identify p with

$(0, 0, 0)$, and identify $-K$ with the z -axis. Regard the surface which K penetrates as the xy -plane. Since K is a transverse knot, it transverses the contact 2-planes positively. Thus at a point $r \in K \cap N$ the positive normal vector \vec{n}_r to the contact plane ξ_r has a negative z -component, i.e., $\vec{n}_r \cdot (0, 0, 1) < 0$. We may assume that contact planes are almost parallel to each other in N . Therefore, at the new hyperbolic point $h \in N$ we have $T_h \Sigma = -\xi_h$. This means that h is a negative hyperbolic point. \square

Since the two end points of a ribbon (resp. clasp) singularity have the same sign (resp. opposite signs), it follows that:

Corollary 3.9. (1) *The resolution of a ribbon singularity creates one positive and one negative hyperbolic points.*

(2) *The resolution of a clasp singularity creates two hyperbolic points of the same sign.*

(3) *The resolution of a branch singularity creates one hyperbolic point. See Figure 17.*

It makes sense to define *the sign* for clasp and branch arcs:

Definition 3.10. (1) If both end points of a clasp arc are positive (negative) intersections of K and Σ , then we say the *sign* of the clasp is *positive (negative)*.

(2) If the end point $p = l \cap K$ of a branch arc is a positive (negative) intersection, then we say the *sign* of the branch arc is *positive (negative)*.

3.6. Construction of the embedded surface Σ_b . In Section 3.3 we have defined a Seifert surface Σ_b for the case $k = 0$.

When $k \neq 0$, Example 3.7 shows that the immersed surface \hat{F}_b has branch, clasp, and ribbon intersections. In this section, we construct an embedded surface Σ_b by resolving these singularities.

When $k > 0$, as shown in Figure 22-(1,2), we can make all the branch, ribbon and clasp arcs transverse to the characteristic foliation $\mathcal{F}_{\hat{F}_b}$. We apply the argument in Section 3.5 and construct an embedded surface Σ_b . Since all the signs of the branch and clasp arcs are negative, Example 3.7 and Corollary 3.9 imply that, when $s > 0$, the resolution of these self-intersections creates, in total, $a_\rho + 2(\frac{1}{2}a_\rho(s-1)) = a_\rho s$ negative hyperbolic singularities. When $s = 0$ there are no branch or clasp intersections, so no new hyperbolic points are created.

When $k < 0$, a similar argument holds.

4. THE SELF LINKING NUMBER

We finally compute the self-linking number $sl(b, [\Sigma_b])$ of b relative to the embedded surface Σ_b .

Theorem 4.1. *Let b be a null-homologous transverse braid in the open book decomposition (A, D^k) satisfying Assumption 2.3. There exists a Seifert surface Σ_b of b which satisfies the formula:*

$$sl(b, [\Sigma_b]) = -n + a_\sigma + a_\rho(1 - s).$$

In particular, when $k \neq 0$, $sl(b, [\Sigma_b])$ does not depend on the choice of Seifert surface and hence we have the following general formula:

$$sl(b) = -n + a_\sigma + a_\rho(1 - s).$$

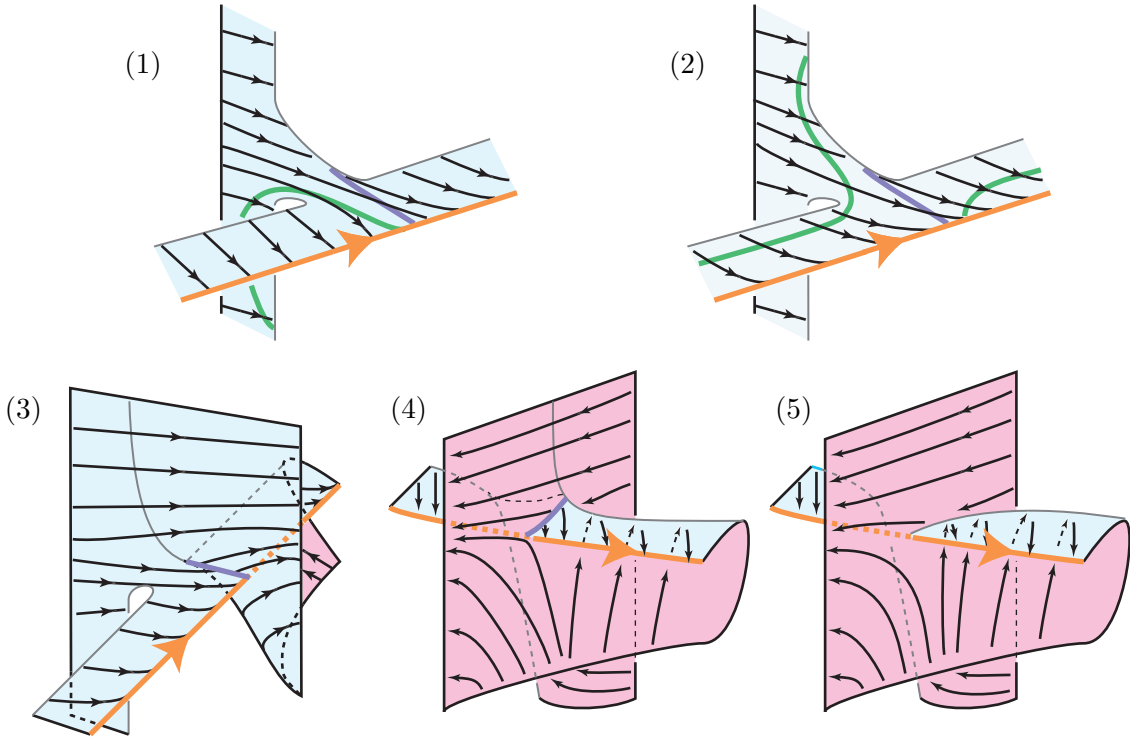


FIGURE 22. Clasp (light green) and branch (dark purple) intersections are transverse to characteristic foliations (top). Characteristic foliation near a branch singularity and its resolution (bottom).

- Remark 4.2.*
- When $k \neq 0$, our manifold $M_{(A, D^k)}$ is a lens space (Claim 2.1) which has $H_2(L(k, q), \mathbb{Z}) = 0$. Therefore, the self linking number does not depend on choice of a Seifert surface and we can denote $sl(b, [\Sigma_b])$ simply by $sl(b)$.
 - The null-homologous condition ensures $a_\rho = 0$ when $k = 0$ (Corollary 2.9).
 - When $a_\rho = 0$ we exactly obtain the Bennequin's formula (1.1).

Proof of Theorem 4.1. Let Σ_b be the surface constructed in Section 3.6.

It is known (see [5] for example) that

$$(4.1) \quad sl(b, [\Sigma_b]) = -(e^+ - e^-) + (h^+ - h^-),$$

where e^+ (e^-) and h^+ (h^-) represent the number of positive (negative) elliptic and positive (negative) hyperbolic singularities of the characteristic foliation \mathcal{F}_{Σ_b} on Σ_b . Let h_σ^+ (h_σ^-) be the number of σ_i 's (σ_i^{-1} 's) which appear in the braid word for b . Then we have $a_\sigma = h_\sigma^+ - h_\sigma^-$, the sign count of hyperbolic singularities on Σ_b given by the bands joining δ -disks as in Figure 9-(1).

Based on Remarks 3.3, 3.5 and Section 3.6, we summarize the count of singularities:

$$\begin{aligned} e^+ &= (n; \text{ on } \delta\text{-disks}) + (s; \text{ on } \omega\text{-disks}) \\ e^- &= (s; \text{ on } \mathcal{D}\text{-disks}) \\ h^+ &= (h_\sigma^+; \text{ on } +\text{bands between } \delta\text{-disks}) + (a_\rho; \text{ on bands between } \delta_n \text{ and } \mathfrak{A}\text{-annuli}) \\ h^- &= (h_\sigma^-; \text{ on } -\text{bands between } \delta\text{-disks}) + (a_\rho s; \text{ by resolution of branches, clasps, ribbons}) \end{aligned}$$

By (4.1) we obtain the desired formula. \square

The Bennequin-Eliashberg inequality [2, 3] states that contact structure (M, ξ) is tight if and only if

$$(4.2) \quad sl(K, [\Sigma]) \leq -\chi(\Sigma)$$

for any (K, Σ) a null-homologous transverse knot and its Seifert surface.

Corollary 4.3. *The contact structure $(M_{(A, D^k)}, \xi_k)$ is tight if and only if for any braid $b \subset (A, D^k)$ inequality $sl(b) \leq -\chi(\Sigma_b)$ holds.*

Proof of Corollary 4.3. As $\chi(\Sigma_b) = (e^+ + e^-) - (h^+ + h^-)$, the inequality $sl(b) \leq -\chi(\Sigma_b)$ is equivalent to $0 \leq h^- - e^- = h_\sigma^- + s(a_\rho - 1)$. Claim 2.2 states that $(M_{(A, D^k)}, \xi_k)$ is tight if and only if $k \geq 0$.

When $k \geq 0$, we have $s(a_\rho - 1) = s(ks - 1) \geq 0$, thus $h^- - e^- \geq 0$.

When $k < 0$, we have $s(a_\rho - 1) < 0$ by Corollary 2.9. Therefore, there exists b for which $h^- - e^- < 0$. \square

Remark 4.4. It is interesting to note that the Bennequin-Eliashberg inequality is *not* satisfied for the immersed surface \hat{F}_b even for the tight cases.

Next, we study behavior of $sl(b, [\Sigma_b])$ under braid stabilizations.

Let b be a null-homologous braid in the open book (A, D^k) . For $\epsilon \in \{+, -\}$ let b_ϵ^γ (resp. $b_\epsilon^{\gamma'}$) denote the braid obtained from b after an ϵ -stabilization about the binding γ (resp. γ'). By Theorem 2.8, braids b, b_+^γ and $b_+^{\gamma'}$ are transversely isotopic regardless of choice of stabilization arc a . Etnyre's [4, Theorem 3.8] implies that if b is a one component link, then a negative stabilization is unique up to transverse isotopy, regardless of choice of arc a , thus $b_-^\gamma = b_-^{\gamma'}$.

Corollary 4.5. *we have:*

$$(4.3) \quad sl(b, [\Sigma_b]) = sl(b_+^\gamma, [\Sigma_{b_+^\gamma}]) = sl(b_-^\gamma, [\Sigma_{b_-^\gamma}]) + 2,$$

$$(4.4) \quad sl(b, [\Sigma_b]) = sl(b_+^{\gamma'}, [\Sigma_{b_+^{\gamma'}}]) = sl(b_-^{\gamma'}, [\Sigma_{b_-^{\gamma'}}]) + 2.$$

Proof of Corollary 4.5. A positive (negative) stabilization about γ changes $n \rightarrow n + 1$ and $a_\sigma \rightarrow a_\sigma + 1$ ($a_\sigma \rightarrow a_\sigma - 1$). Applying Theorem 4.1, we get (4.3).

For (4.4), as we have seen in the proof of Proposition 2.6, by a positive (negative) braid stabilization, we have the following data change:

$$\begin{aligned} n &\rightarrow n + 1, & a_\sigma &\rightarrow a_\sigma + 1 + 2a_\rho, & s &\rightarrow s + 1, & a_\rho &\rightarrow a_\rho + k, \\ (n &\rightarrow n + 1, & a_\sigma &\rightarrow a_\sigma - 1 + 2a_\rho, & s &\rightarrow s + 1, & a_\rho &\rightarrow a_\rho + k). \end{aligned}$$

Applying Theorem 4.1, we have

$$\begin{aligned} sl(b_+^{\gamma'}, [\Sigma_{b_+^{\gamma'}}]) &= -(n+1) + (a_\sigma + 1 + 2a_\rho) + (a_\rho + k)(1 - (s+1)) \\ &= -n + a_\sigma + a_\rho(1 - s) \\ &= sl(b, [\Sigma_b]). \end{aligned}$$

A similar computation leads to $sl(b_-^{\gamma'}, [\Sigma_{b_-^{\gamma'}}]) + 2 = sl(b, [\Sigma_b])$. □

5. SEIFERT FIBERED MANIFOLDS

Let S be an oriented pair of pants with boundary circles γ_i for $i = 1, 2, 3$. See Figure 23. Let α_i be circles parallel to γ_i . Denote the positive Dehn twist about α_i by D_i . Let

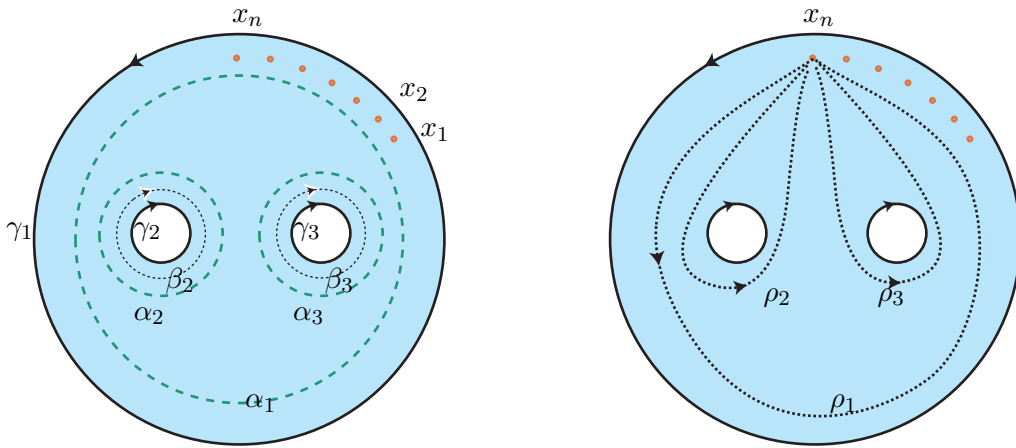


FIGURE 23. A pair of pants S .

k_i be an integer, $i = 1, 2, 3$. In this section we study closed braids in the open book decomposition $(S, D_1^{k_1} \circ D_2^{k_2} \circ D_3^{k_3})$. The corresponding manifold, which we denote by $M_{k_1, k_2, k_3} (= M)$, is a Seifert fibered space over the orbifold of signature $(0, k_1, k_2, k_3)$. A similar argument as in the proof of Claim 2.1 tells that M_{k_1, k_2, k_3} has surgery descriptions as in Figure 24. In Sketch (1), the two circles with slope 0 represent the unlinked unknots

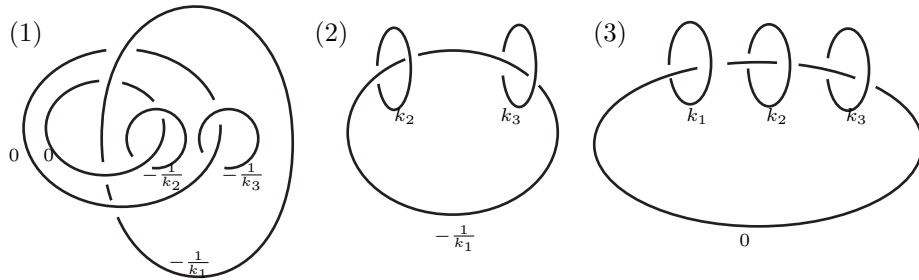


FIGURE 24. Surgery descriptions for M_{k_1, k_2, k_3} .

through the holes of S , γ_2 and γ_3 (cf. the unknot U in the proof of Claim 2.1). Slam-dunk operations are applied in the passage Sketch (1) \rightarrow (2) \rightarrow (3). Etnyre-Ozbagci [7, page 3136] implies:

$$(5.1) \quad H_1(M_{k_1, k_2, k_3}; \mathbb{Z}) = \langle c_2, c_3 \mid (k_1 + k_2)c_2 + k_1c_3 = k_1c_2 + (k_1 + k_3)c_3 = 0 \rangle,$$

where $c_j \in \pi_1(S)$ is the standard generator corresponding to the boundaries γ_j of S . We remark that $H_2(M; \mathbb{Z})$ is non-trivial in general, which is distinct from the lens spaces.

Proposition 5.1. *Let ξ_{k_1, k_2, k_3} denote the contact structure for M_{k_1, k_2, k_3} compatible with the open book $(S, D_1^{k_1} \circ D_2^{k_2} \circ D_3^{k_3})$ via the Giroux correspondence [9]. Then ξ_{k_1, k_2, k_3} is tight if and only if $k_1, k_2, k_3 \geq 0$.*

Proof. If $k_1 = k_2 = k_3 = 0$, then $M_{0,0,0} = (S^1 \times S^2) \# (S^1 \times S^2)$. Etnyre-Honda explain in the proof of [6, Lemma 3.2] that $\xi_{0,0,0}$ is Stein fillable, hence tight. In fact, it is the unique tight structure, which is due to Eliashberg [3].

If $k_1, k_2, k_3 \geq 0$ and $(k_1, k_2, k_3) \neq (0, 0, 0)$, Etnyre-Honda [6, Lemma 3.2] tells that ξ_{k_1, k_2, k_3} is tight.

If one of k_i is negative, say $k_1 < 0$, then a properly embedded boundary *non-parallel* essential arc whose both ends sit on γ_1 is a sobering arc, see [10, Definition 3.2]. Thus Goodman's [10, Theorem 1.2] implies that ξ_{k_1, k_2, k_3} is overtwisted. \square

Let K be a null-homologous transverse knot in (M, ξ_{k_1, k_2, k_3}) . By Theorem 1.3 we can identify K with a closed n -braid b in $(S, D_1^{k_1} \circ D_2^{k_2} \circ D_3^{k_3})$.

Assumption 5.2. *Applying braid isotopy (transverse isotopy), we may assume that there exist points x_1, \dots, x_n (orange dots in Figure 23) sitting between γ_1 and α_1 such that $b \cap (S \times \{0\}) = \{x_1, \dots, x_n\}$.*

Let σ_i be a mapping class of S with n fixed points x_1, \dots, x_n , exchanging x_i and x_{i+1} counter clockwise. Let ρ_j ($j = 1, 2, 3$) be a mapping class which moves x_n around the boundary circle γ_j as described in Figure 23. Since σ_i 's and ρ_j 's are generators of the mapping class group and $\rho_1 = \rho_2 + \rho_3$, it follows that:

Proposition 5.3. *An n -strand closed braid in the open book $(S, D_1^{k_1} \circ D_2^{k_2} \circ D_3^{k_3})$ can be written in letters $\{\sigma_1, \dots, \sigma_{n-1}, \rho_2, \rho_3\}$.*

We define symbols a_σ, a_{ρ_i} , and s_i :

Definition 5.4. Let a_σ be the exponent sum of σ_i 's in the braid word for b . Let a_{ρ_i} ($i = 2, 3$) be the exponent sum of ρ_i in the braid word for b . Since b is null-homologous, we have $0 = [b] = a_{\rho_2}c_2 + a_{\rho_3}c_3$ in $H_1(M; \mathbb{Z})$. By equation (5.1), there exist $s_2, s_3 \in \mathbb{Z}$, so that

$$0 = [b] = s_2 \{(k_1 + k_2)c_2 + k_1c_3\} + s_3 \{k_1c_2 + (k_1 + k_3)c_3\}.$$

Therefore,

$$(5.2) \quad [a_{\rho_2}, a_{\rho_3}] = [s_2, s_3] \begin{bmatrix} k_1 + k_2 & k_1 \\ k_1 & k_1 + k_3 \end{bmatrix}.$$

For special cases;

- (1) when $k_1 = k_2 = 0$ and $k_3 \neq 0$, we set $s_2 = 0$, i.e., $a_{\rho_2} = 0$ and $a_{\rho_3} = s_3k_3$,
- (2) when $k_1 = k_3 = 0$ and $k_2 \neq 0$, we set $s_3 = 0$, i.e., $a_{\rho_3} = 0$ and $a_{\rho_2} = s_2k_2$,

(3) when $k_1 = k_2 = k_3 = 0$, we set $s_2 = s_3 = 0$, i.e., $a_{\rho_2} = a_{\rho_3} = 0$.

Lemma 5.5. *We may assume that $s_2, s_3 \geq 0$ and that a_{ρ_2}, a_{ρ_3} satisfy (5.2).*

Proof. A similar argument as in the proof of Proposition 2.6 applies. Recall that a positive braid stabilization preserves the transverse knot type (Theorem 2.8). Since the point x_n is between γ_1 and α_1 , positive stabilizations of b about γ_2 (resp. γ_3) for α -times (resp. β -times), where $\alpha, \beta \geq 0$, change a_{ρ_i} in the following way:

$$\begin{aligned} a_{\rho_2} &\mapsto a_{\rho_2} + \alpha(k_1 + k_2), \quad a_{\rho_3} \mapsto a_{\rho_3} + \alpha k_1, \\ &\text{(resp. } a_{\rho_2} \mapsto a_{\rho_2} + \beta k_1, \quad a_{\rho_3} \mapsto a_{\rho_3} + \beta(k_1 + k_3)). \end{aligned}$$

By (5.2), s_i also changes as;

$$\begin{aligned} s_2 &\mapsto s_2 + \alpha \quad \text{if } k_1 + k_2 \neq 0 \text{ or } k_1 \neq 0, \\ &\text{(resp. } s_3 \mapsto s_3 + \beta \quad \text{if } k_1 + k_3 \neq 0 \text{ or } k_1 \neq 0). \end{aligned}$$

Therefore taking α, β sufficiently large, we can make $s_2, s_3 \geq 0$, even for the special three cases in Definition 5.4. \square

Now we state our main result of this section:

Theorem 5.6. *Let b be a null-homologous closed braid in $(S, D_1^{k_1} \circ D_2^{k_2} \circ D_3^{k_3})$ satisfying Assumption 5.2 and Lemma 5.5. There is a Seifert surface Σ_b of b for which the following holds:*

$$sl(b, [\Sigma_b]) = -n + a_\sigma + a_{\rho_2}(1 - s_2) + a_{\rho_3}(1 - s_3) - (s_2 + s_3)k_1.$$

Proof. We construct an embedded surface \tilde{F}_b after Sections 3.1 and 3.2.

- Construct n -copies of the δ -disk (cf. Figure 8).
- Join them by twisted bands for each σ_j^\pm in the braid word (cf. Figure 9-(1)).
- Attach \mathfrak{A} -annuli for each ρ_2^\pm, ρ_3^\pm in the braid word (cf. Figure 9-(2)).
- Attach vertical nested annuli to remove redundant boundaries (cf. Figure 11).

This procedure is more subtle than that of annulus open book case.

If $k_1, k_2, k_3 \geq 0$ or $k_1, k_2, k_3 \leq 0$ then attach vertical nested annuli near the bindings γ_2 and γ_3 following the algorithm described in the proof of Proposition 3.1. The boundary of the resulting surface, \tilde{F}_b , has

$$\begin{aligned} \partial \tilde{F}_b &= b \cup \{|(s_2 + s_3)k_1 + s_2k_2| \text{ copies of } \epsilon(k_2)\beta_2\} \\ &\quad \cup \{|(s_2 + s_3)k_1 + s_3k_3| \text{ copies of } \epsilon(k_3)\beta_3\} \end{aligned}$$

where β_i is the oriented circle as in Figure 23 and $\epsilon(k_i)$ is the sign of k_i .

Otherwise, by symmetry of the pants surface we may assume that (i) $k_1, k_2 \geq 0$ and $k_3 < 0$, or (ii) $k_1, k_2 \leq 0$ and $k_3 > 0$. For either case, we change the braid word by adding dummy letters that preserves the transverse knot type:

$$(5.3) \quad b \mapsto (b \rho_3^{-s_3k_3}) (\rho_3^{s_3k_3})$$

Attach vertical nested annuli to the first part $b\rho_3^{-s_3k_3}$, without touching the remaining part $\rho_3^{s_3k_3}$, until all their boundary circles of the \mathfrak{A} -annuli have the same direction. The boundary of the resulting surface, \tilde{F}_b , has

$$\begin{aligned} \partial \tilde{F}_b &= b \cup \{(s_2 + s_3)|k_1| \text{ copies of } \epsilon(k_2)(\beta_2 + \beta_3)\} \\ &\quad \cup \{s_2|k_2| \text{ copies of } \epsilon(k_2)\beta_2\} \cup \{s_3|k_3| \text{ copies of } \epsilon(k_3)\beta_3\}. \end{aligned}$$

We require the operation (5.3) so that \mathcal{D} -disks introduced below can be compatible with the monodromy of the open book. Note that if the signs of k_2 and k_3 are different

$$|a_{\rho_2}| = |(s_2 + s_3)k_1 + s_2k_2| = (s_2 + s_3)|k_1| + s_2|k_2|,$$

but

$$|a_{\rho_3}| = |(s_2 + s_3)k_1 + s_3k_3| \neq (s_2 + s_3)|k_1| + s_3|k_3|.$$

Compare Figure 25, where k_i 's have the same sign, and Figure 26, where $k_1, k_2 > 0$ and $k_3 < 0$. Their right bottom parts are different.

Next step is to construct an immersed surface \hat{F}_b . If $k_1 = k_2 = k_3 = 0$ we define $\hat{F}_b = \tilde{F}_b$. Otherwise apply the following:

- If $k_1 = 0$ we skip this step.
If $k_1 \neq 0$, join the top two \mathfrak{A} -annuli around γ_2 and γ_3 by a band, called a *bridge band* as in Figures 27, 25. The bridge band connects the β_2 circle and the β_3 circle of \tilde{F}_b . If the θ -coordinate (height) of the \mathfrak{A} -annulus around γ_2 is larger (resp. smaller) than the one around γ_3 , then the bridge band is attached to β_2 from below (resp. above) and to β_3 from above (resp. below). As a consequence, the bridge band does not tangent to the pages of the open book.
Repeat this for the first $(s_2 + s_3)|k_1|$ pairs of \mathfrak{A} -annuli from the top.
- If $k_1 = k_2 = 0$ we skip this step.
Otherwise, put s_2 copies of the ω -disk, $\omega_1, \dots, \omega_{s_2}$, about γ_2 (dark pink in Figure 25). Denote the \mathfrak{A} -annuli around γ_2 from the top by $\mathfrak{A}_1, \dots, \mathfrak{A}_{|k_1|(s_2+s_3)+|k_2|s_2}$. Connect the disk ω_i with $|k_1| + |k_2|$ copies of \mathfrak{A} -annulus;

$$\begin{aligned} & \mathfrak{A}_{s_3+i}, \mathfrak{A}_{2s_3+s_2+i}, \dots, \mathfrak{A}_{|k_1|s_3+(|k_1|-1)s_2+i}, \\ & \mathfrak{A}_{|k_1|(s_3+s_2)+i}, \mathfrak{A}_{|k_1|(s_3+s_2)+s_2+i}, \dots, \mathfrak{A}_{|k_1|(s_3+s_2)+(|k_2|-1)s_2+i}, \end{aligned}$$

(when $k_1 = 0, k_2 \neq 0$, they are $\mathfrak{A}_i, \mathfrak{A}_{s_2+i}, \dots, \mathfrak{A}_{(|k_2|-1)s_2+i}$,

when $k_1 \neq 0, k_2 = 0$, they are $\mathfrak{A}_{s_3+i}, \mathfrak{A}_{2s_3+s_2+i}, \dots, \mathfrak{A}_{|k_1|s_3+(|k_1|-1)s_2+i}$)

by using the twisted bands. Depending on the signs of k_1 and k_2 , the twisted band is attached differently as described in Figure 13.

- Attach s_2 copies of \mathcal{D} -disk about γ_1 to the \mathfrak{A} -annuli around γ_2 .
- Similarly, attach s_3 copies of ω -disk (lighter shaded in Figure 25) about γ_3 , add $|k_1| + |k_3|$ copies of twisted bands, and s_3 copies of \mathcal{D} -disk.

Finally we have obtained an immersed surface \hat{F}_b with boundary b .

The following two lemmas investigate singularities of the characteristic foliation.

Lemma 5.7. *If $k_1 > 0$ (resp. $k_1 < 0$) then the characteristic foliation for each bridge band has a single negative (resp. positive) hyperbolic singularity. See Figure 27.*

Proof. Let p_i ($i = 2, 3$) be a point on the binding γ_i . Assume $p'_i \in \beta_i$ is a point close to p_i and the bridge band connects p'_2 and p'_3 , see Figure 27. At p_i , the contact plane intersects γ_i positively. Along the line segment from p'_2 to p'_3 , the contact planes rotate $(180 - \epsilon)^\circ$ counterclockwise. The contact plane is tangent to the bridge band at a single point somewhere between p'_2 and p'_3 , where the hyperbolic singularity occurs. If $k_1 > 0$ (resp. $k_1 < 0$), the positive (negative) side of the band is facing up to the reader, thus the sign of the hyperbolic point is positive (negative). \square

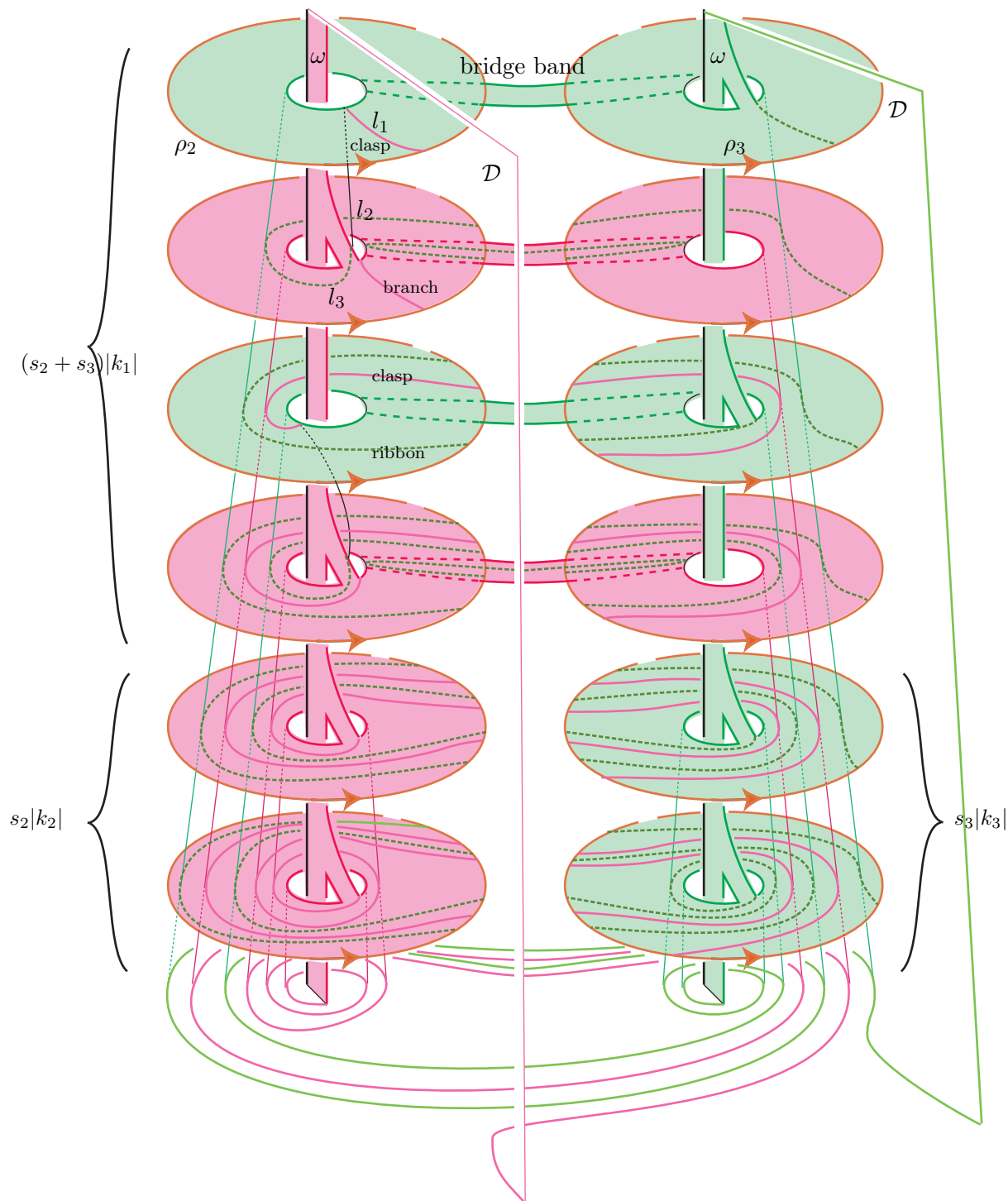


FIGURE 25. An immersed surface. $k_1 = k_2 = k_3 = 2$. $s_2 = s_3 = 1$. Bridge bands are attached from above/below \mathcal{A} -annuli depending on their θ -heights.

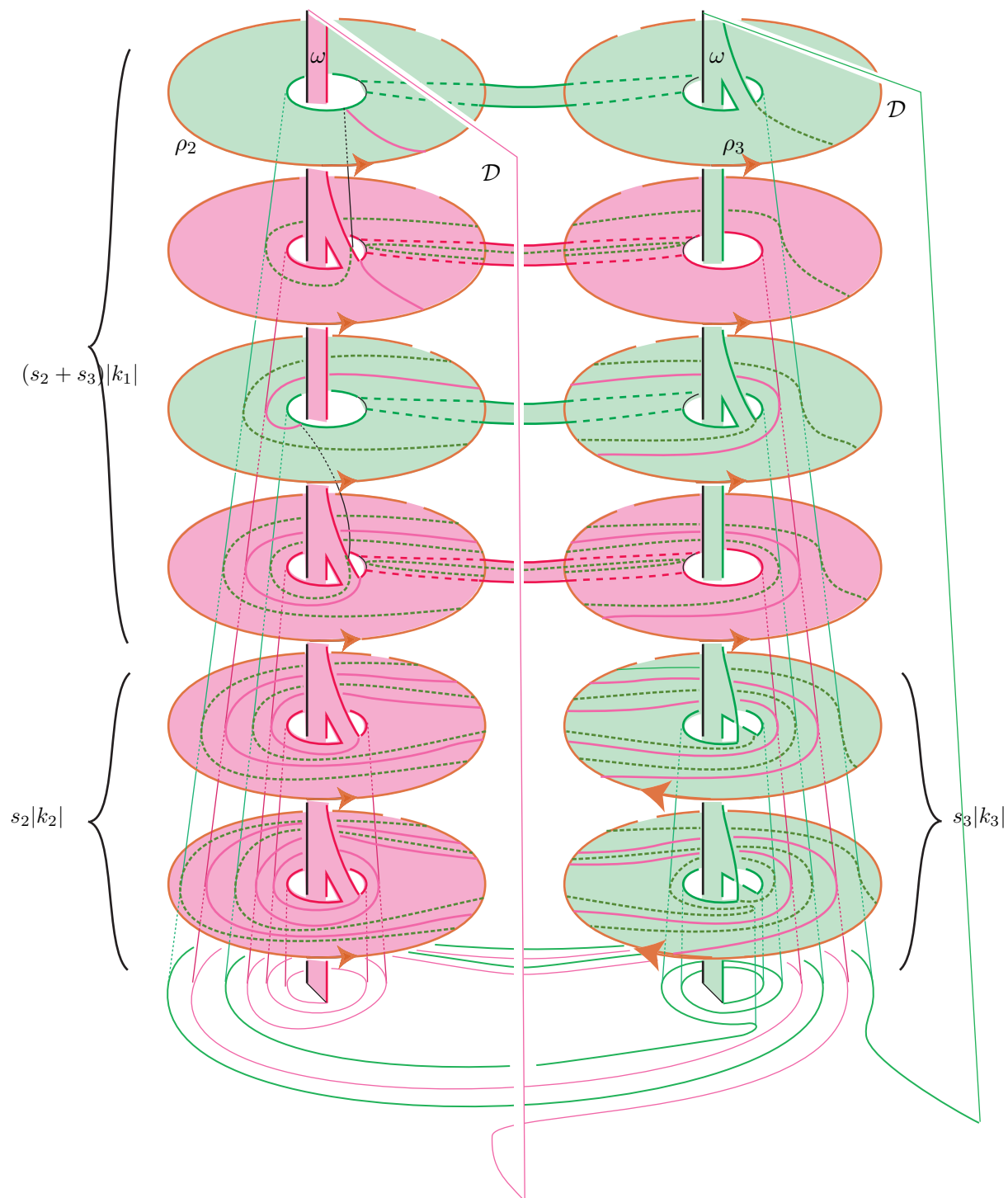
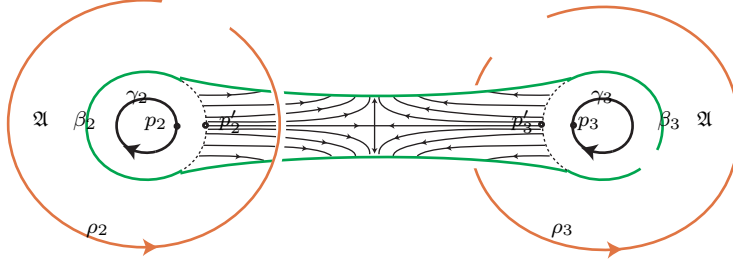


FIGURE 26. An immersed surface. $k_1 = k_2 = 2, k_3 = -2, s_2 = s_3 = 1$.


 FIGURE 27. Characteristic foliation on a bridge band when $k_1 > 0$.

Lemma 5.8. *All the singularities of the characteristic foliation for $(\hat{F}_b \setminus \tilde{F}_b)$, the union of ω -disks, twisted bands and \mathcal{D} -disks, are elliptic. Moreover, the algebraic count $e^+ - e^-$ of elliptic singularities for the ω -disks (resp. \mathcal{D} -disks) is $s_2 + s_3$, (resp. $-s_2 - s_3$).*

Proof. As seen in the proof of Lemma 3.2, there are no hyperbolic singularities on the twisted bands. \square

We continue the proof of Theorem 5.6.

Figure 25 exhibits branch, clasp and ribbon intersections of \hat{F}_b . For example, in Figure 25, the union of arcs $l_1 \cup l_2 \cup l_3$ is a clasp intersection. Each pair among the $s_2 + s_3$ \mathcal{D} -disks about γ_1 gives rise to $|k_1|$ clasp intersections. Additionally, each pair among the s_2 \mathcal{D} -disks about γ_1 attached to curves near γ_2 gives rise to $|k_2|$ clasp intersections, and each pair among the s_3 \mathcal{D} -disks about γ_1 attached to curves near γ_3 gives rise to $|k_3|$ clasp intersections. In total, there are

$$\begin{aligned} & |k_1| \binom{s_2 + s_3}{2} + |k_2| \binom{s_2}{2} + |k_3| \binom{s_3}{2} \\ &= \binom{s_2}{2} (|k_1| + |k_2|) + \binom{s_3}{2} (|k_1| + |k_3|) + s_2 s_3 |k_1| \end{aligned}$$

clasp intersections. Signs are assigned to each intersection according to Definition 3.10. If we count them algebraically,

$$(5.4) \quad \text{algebraic number of branches} = -s_2(k_1 + k_2) - s_3(k_1 + k_3).$$

$$(5.5) \quad \text{algebraic number of clasps} = -\binom{s_2}{2}(k_1 + k_2) - \binom{s_3}{2}(k_1 + k_3) - s_2 s_3 k_1.$$

Resolving all the intersection arcs, we obtain an embedded surface Σ_b .

By Proposition 3.8 and Corollary 3.9, the resolution of branch, clasp and ribbon intersections create additional hyperbolic singularities. The total algebraically counted number of such hyperbolic points is:

$$(5.6) \quad (5.4) + 2 \times (5.5) = -\{(s_2 + s_3)^2 k_1 + s_2^2 k_2 + s_3^2 k_3\}.$$

In summary we have:

$$\begin{aligned}
e^+ &= (n; \delta\text{-disks}) + (s_2 + s_3; \omega\text{-disks}), \\
e^- &= (s_2 + s_3; \mathcal{D}\text{-disks}), \\
h^+ - h^- &= (a_\sigma; \text{bands between } \delta\text{-disks}) + (a_{\rho_2} + a_{\rho_3}; \text{bands between } \delta_n \text{ and } \mathfrak{A}\text{-annuli}) \\
&\quad - (k_1(s_2 + s_3); \text{bridge bands; Lemma 5.7}) \\
&\quad - ((s_2 + s_3)^2 k_1 + s_2^2 k_2 + s_3^2 k_3; \text{resolution of branches, clasps, ribbons (5.6)}) \\
&\stackrel{(5.2)}{=} a_\sigma + a_{\rho_2} + a_{\rho_3} - s_2(a_{\rho_2} + k_1) - s_3(a_{\rho_3} + k_1) \\
&= a_\sigma + a_{\rho_2}(1 - s_2) + a_{\rho_3}(1 - s_3) - (s_2 + s_3)k_1.
\end{aligned}$$

Finally we have

$$\begin{aligned}
sl(b, [\Sigma_b]) &= -(e^+ - e^-) + (h^+ - h^-) \\
&= -n + a_\sigma + a_{\rho_2}(1 - s_2) + a_{\rho_3}(1 - s_3) - (s_2 + s_3)k_1.
\end{aligned}$$

□

REFERENCES

1. Alexander, J.W. *A Lemma on Systems of Knotted Curves* Proc Natl Acad Sci U S A, March 1923, 9(3), 93–95.
2. Bennequin, Daniel. *Entrelacements et équations de Pfaff*, Astérisque, 107-108, (1983) 87–161.
3. Eliashberg, Yakov. *Contact 3-manifolds twenty years since J. Martinet’s work*. Ann. Inst. Fourier (Grenoble) 42 (1992), no. 1-2, 165–192.
4. Etnyre, John B. *Transversal torus knots*. Geom. Topol. 3 (1999), 253–268.
5. Etnyre, John B. *Legendrian and transversal knots*. Handbook of knot theory, 105–185, Elsevier B. V., Amsterdam, 2005.
6. Etnyre, John B; Honda, Ko. *On symplectic cobordisms* Math. Ann. 323 (2002) no. 1, 31-39
7. Etnyre, John B.; Ozbagci, Burak. *Invariants of contact structures from open books*. Trans. Amer. Math. Soc. 360 (2008), no. 6, 3133–3151.
8. Geiges, Hansjörg. *An introduction to contact topology*. Cambridge Studies in Advanced Mathematics, 109. Cambridge University Press, Cambridge, 2008.
9. Giroux, Emmanuel. *Contact geometry: from dimension three to higher dimensions*. Proceedings of the International Congress of Mathematicians, Vol. II (Beijing, 2002), 405–414, Higher Ed. Press, Beijing, 2002.
10. Goodman, Noah. *Overtwisted open books from sobering arcs*. Algebr. Geom. Topol. 5 (2005), 1173–1195.
11. Honda, Ko. *On the classification of tight contact structures I*. Geom. Topol. 4 (2000), 309–368.
12. Ozbagci, Burak; Stipsicz, András I. *Surgery on contact 3-manifolds and Stein surfaces*. Bolyai Society Mathematical Studies, 13. Springer-Verlag, Berlin; János Bolyai Mathematical Society, Budapest, 2004.
13. Pavelescu, Elena. *Braids and Open Book Decompositions*. University of Pennsylvania, Ph.D. thesis.

DEPARTMENT OF MATHEMATICS, THE UNIVERSITY OF IOWA, IOWA CITY, IOWA 52240
E-mail address: kawamuro@uiowa.edu

DEPARTMENT OF MATHEMATICS, RICE UNIVERSITY, HOUSTON, TEXAS 77005
E-mail address: Elena.Pavelescu@rice.edu